ISEIS

Journal of Environmental Informatics 45(1) 27-41 (2025)

Journal of Environmental Informatics

www.iseis.org/jei

Assessment of Uncertainty Propagation from Climate Modeling to Hydrologic Forecasting under Changing Climatic Conditions

H. J. Wu[1], X. D. Ye[2 *], B. Y. Zhang[1], and B. Chen[1 *]

[1] *Northern Region Persistent Organic Pollution Control (NRPOP) Laboratory, Memorial University of Newfoundland, Faculty of Engineering and Applied Science, St. John's, NL A1B 3X5, Canada*

[2] *Key Laboratory for Coastal Marine Eco-Environment Process and Carbon Sink of Hainan province, Yazhou Bay Innovation Institute, College of Ecology and Environment, Hainan Tropical Ocean University, Sanya 572000, China*

Received 19 June 2023; revised 30 September 2023; accepted 06 August 2024; published online 03 January 2025

ABSTRACT. The changing climate has a profound impact on the hydrological cycle and water balance, complicating water resources management. General circulation models (GCMs) and downscaling methods have been widely employed to reflect and quantify climate change effects in hydrological studies. The uncertainties associated with GCMs, downscaling methods, and hydrological modeling mutually interact, significantly amplifying the complexity of uncertainty analysis. To address this challenge, we proposed the Integrated simulation-based evaluation system for uncertainty propagation analysis (ISES-UPA) method, specifically designed to assess the uncertainty propagation effect from statistical downscaling and hydrological modeling. This study aims to utilize ISES-UPA to inves-tigate the effects and contributions of different uncertainty components to the total uncertainty in hydrological modeling under changing climatic conditions. Successfully applied to a real case study in Sichuan, China, the results reveal that the total propagated uncertainty significantly surpasses the simple addition of other sources (e.g., about 2.15 times from statistical downscaling and about 4.44 times from hydrological modeling on average). By using ISES-UPA, individual and combined uncertainties from statistical downscaling and hydrological modeling can be compared and quantified, thereby enhancing the reliability of hydrological studies under changing climate conditions.

Keywords: climate change, hydrological modeling, statistical downscaling, uncertainty propagation effects, uncertainty analysis

1. Introduction

The increasing concentration of greenhouse gas emissions is widely recognized as the primary catalyst for climate change. Extensive human activities, mainly including the burning of fossil fuels and changes in land cover and use, are major contributors to the increase in greenhouse gas emissions (Wu and Chen, 2014; Tian et al., 2020). The Intergovernmental Panel on Climate Change (IPCC) claimed that climate change had considerable impacts on water basins and regions due to changes in air temperatures and precipitation (IPCC, 2007; Chen and Niu, 2020). Consequently, researchers have increasingly turned their attention to hydrological studies under changing climate conditions to quantify the impacts of climate change.

Hydrological models are crucial in understanding hydrological processes and making hydrological predictions for different purposes (Lindenschmidt and Rokaya, 2019; Chen et al., 2011). A large number of hydrological models have been developed and applied to a variety of areas, such as flood control (Lu et al., 2019; Dong et al., 2020; Anteneh et al., 2023), water resources management (Rodríguez et al., 2019; Yang et al., 2022), water quality control (Shrestha and Wang, 2020; Zhang et al., 2021; Bui and Pham, 2023), and climate change studies (Dang et al., 2020; Mei et al., 2021). Among different hydrological models, distributed hydrological models have advantages in capturing the spatial variability of watersheds. However, their applications are usually constrained due to the need for high-resolution distributed variables and inputs and the high demand for computational capacity (Lucas-Picher et al., 2020). To ensure the reliability and accuracy of hydrological modeling, proper model calibration and uncertainty analysis need to be carefully conducted.

Due to the complexity of distributed hydrological models, uncertainty analysis is always challenging in simulation and prediction (Jing et al., 2017). The sources of uncertainty and classification of uncertainty have been discussed in multiple literature for hydrological studies (Warmink et al., 2010; Bosshard et al., 2013; Wu et al., 2013; McMillan et al., 2018). As one of the most critical uncertainty sources, climate input data (e.g., precipitation and temperature) required by hydrological models introduce additional uncertainties to the simulation system, especially when considering the effect of climate change (Li et al., 2018). As the climate is a highly non-linear natural system, predicting climate scenarios inevitably involves different sources

* Corresponding author. Tel: +86 17602406401.
E-mail address: owkwork@163.com (X. D. Ye).

* Corresponding author. Tel: +1 (709) 864-8958; Fax: +1 (709) 864-4042.
E-mail address: bchen@mun.ca (B. Chen).

ISSN: 1726-2135 print/1684-8799 online
 doi:10.3808/jei.202500530

of uncertainty (Chaudhuri and Srivastava, 2017). When accounting for the impacts of climate change, the difficulties and complexities of uncertainty quantification are further magnified when climate data are incorporated as inputs for hydrological models.

General circulation models (GCMs) have been developed and utilized to simulate the physical processes to estimate the impacts of the continuously increasing greenhouse gas concentration in the atmosphere on future climate change (DeFries et al., 2023). As mathematical representations, GCMs are widely used for various modeling purposes to reflect future climate features. However, the output of GCMs cannot be directly used as the input to regional hydrological models due to the mismatch of the spatial resolution. Previous studies have demonstrated that using the coarse-resolution GCM outputs for regional hydrological cases yielded unrealistic hydrological results with bias (Wu et al., 2017). Accordingly, downscaling methods have been developed to address the spatial and temporal resolution mismatch, enabling appropriate representations of GCMs outputs in hydrological modeling studies (Nourani et al., 2019). Nonetheless, different sources of uncertainty were involved while downscaling GCMs outputs and different types of uncertainty (e.g., parameter uncertainty model structure uncertainty) during hydrological modelling. Adding to the system will increase the complexity. It is known that different uncertainty sources enforced the total uncertainty hard to be quantified in a hydrological modeling study when employing downscaled GCMs results. Several previous attempts have been made to evaluate uncertainty associated with climate change and hydrological modeling: Maurya et al. (2023) assessed the performance of six GCMs models and coupled GCMs with the SWAT model to forecast future average monthly and annual streamflow for investigating the impact of climate change on Mahi River Basin. Miao et al. (2023) conducted a study to evaluate the runoff changes using outputs of Coupled Model Intercomparison Projects (CMIPs) and decompose the uncertainty from three main sources: internal variability, model uncertainty, and scenario uncertainty. The effect of different uncertainty sources has been evaluated and the results indicate model uncertainty is the major source of uncertainty for CMIPs, spatially. Fallah and Orth (2020) presented a study investigating uncertainty propagates from precipitation data sets into hydrological modeling. The results revealed a strong dependency of simulated runoff on precipitation accuracy, particularly in wet regions. Rakhimova et al. (2020) utilized a multi-model ensemble of six GCMs to assess spatio-temporal variations in precipitation and temperature under representative concentration pathways for future periods. Trolle et al. (2019) identified and ranked uncertainty sources on the future aquatic ecosystems with multiple climate models, land use scenarios and eco-hydrological models. Her et al. (2019) demonstrated the uncertainties in the hydrological analysis of climate changes by multiple climate models and multi-parameter ensemble models. Sharma et al. (2018) assessed uncertainties of hydro-climate variables in India considering multiple downscaling techniques, GCMs and their combined effects. Vetter et al. (2017) evaluated the uncertainty sources in projected hydrological changes in 12 large-scale river basins under changing climate conditions. Krysanova et al. (2017) compared the impacts of climate change with 9 hydrological models for 12 river basins and quantified the uncertainty sources. Van Beusekom et al. (2016) evaluated uncertainties arising from GCMs and their effects on water resources in a tropical island system using ten downscaled GCMs under two greenhouse gas emission scenarios.

As shown above, some previous studies have investigated the impacts of uncertainty arising from various GCMs, emission scenarios, downscaling methods, land-use development, and hydrological models. However, most of these studies' primarily focus on analyzing the future projections of climate and hydrological conditions along with their associated uncertainties (Bennett et al., 2012; Shen et al., 2018; Jin et al., 2019; Wu et al., 2019; Zhu et al., 2019). Understanding and quantifying the contributions of various sources of uncertainty is both meaningful and challenging. Upon reviewing the previous studies and other related literature, it becomes evident that assessing the contributions of uncertainties from various sources within an integrated framework is necessary and useful for understanding uncertainty propagation. However, limited studies have proposed reliable procedures to decompose total uncertainty into various components (Ahmadalipour et al., 2018). Previously, we conducted a study to assess the uncertainty propagation effect from statistical downscaling to hydrological modeling, concentrating solely on the single uncertainty source - statistical downscaling (Wu et al., 2019). To further improve the understanding of uncertainty propagation effect, in this study, uncertainty from hydrological modeling has been incorporated and combined with uncertainty from statistical downscaling, significantly increasing the complexity. Therefore, it is essential to develop an approach that can facilitate a scientific comparison and evaluation of the impacts of uncertainty propagation stemming from various uncertainty components. We propose the integrated simulation-based evaluation system for uncertainty propagation analysis (ISES-UPA) method for solving these challenges. The major contribution of this study lies in decomposing the contribution of different uncertainty components to total uncertainty and quantitatively evaluating the uncertainty propagation effect under changing climatic conditions. A real case study in the upstream of the Wenjing River watershed in Sichuan, China, was conducted to demonstrate the feasibility of the proposed method. The result analysis and contributions of different uncertainty sources were further evaluated and discussed.

2. Methodology

This research introduces the integrated simulation-based evaluation system for uncertainty propagation analysis (ISES-UPA) to quantify the effects of different uncertainty components on the total propagated uncertainty arising from statistical downscaling. The study begins by quantifying the uncertainty associated with statistical downscaling and hydrological modeling separately. Subsequently, these two sources of uncertainty are combined during new hydrological simulations for investigating the total propagated uncertainty. Then, the contributions of different uncertainty components are further evaluated through the proposed ISES-UPA method. The framework of the proposed method is shown in Figure 1, and the significant steps/components are described in the following sections.

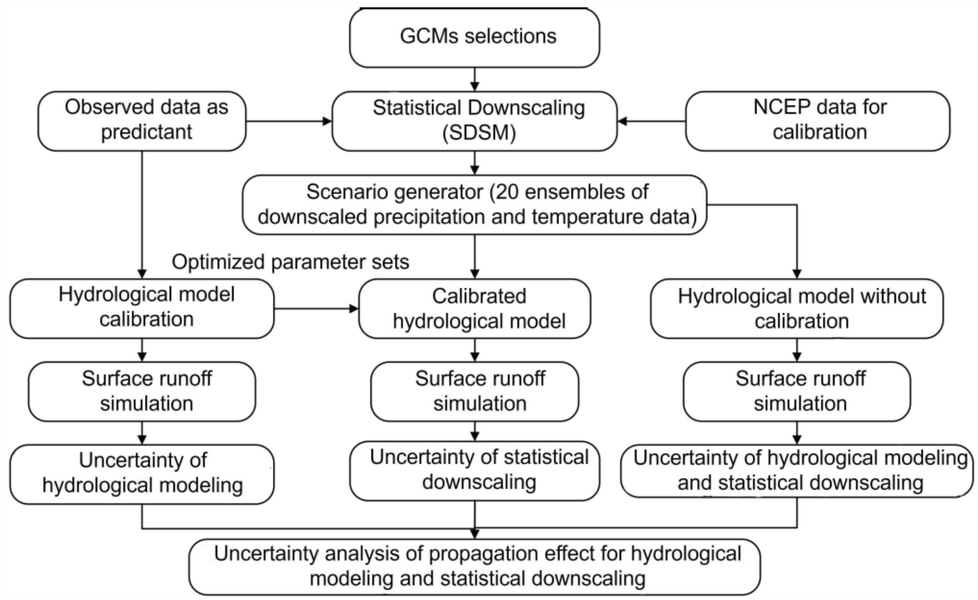

Figure 1. The flowchart for evaluating the propagated uncertainty effects from hydrological modeling and statistical downscaling.

2.1. Study Area GCM Selection

GCMs were developed and considered to be able to provide credible predictions and projections for climate changes over the next 100 years (Sa'adi et al., 2020). Through downscaling processes, the large-scale GCM outputs can be downscaled to the local scale for the use of hydrological models for prediction purposes. Currently, there are many GCMs available. In the first step for real case studies, suitable GCMs should be considered for the specific study area. Due to the accessibility or availability of data, only several GCMs are useful/suitable for certain areas. Different models can be selected according to different simulation purposes as well. The A2 scenario family illustrates a diverse world with a growing global population characterized by unbalanced and regionally focused economic development. Notably, the A2 family is the only scenario projecting net Anthropogenic CO_2 emissions through 2100. Given data availability and the A2 scenario's representation of extreme changes in precipitation and temperatures by the century's end (considered as the worst-case scenario), the Hadley Centre Coupled Model 3 (HadCM3) for A2 scenario (H3A2a) was selected for downscaling in this study (Nakicenovic et al., 2000; Gudmundsson, 2012; Samadi et al., 2012; Wu et al., 2019).

2.2. Statistical Downscaling (SDSM)

Traditionally, downscaling methods have been classified into two major categories: dynamic downscaling and statistical downscaling. Due to high computational demand and cost, dynamic downscaling methods are available for limited areas and studies (Chadwick et al., 2011; Dai et al., 2020; Tapiador et al., 2020). Statistical downscaling is more suitable for the studies of climate change impacts due to its straightforward design methodology, computational ease and ability to produce synthetic datasets of any desired length (Chadwick et al., 2011). Different from dynamic downscaling, the statistical downscaling methods are based on a statistical relationship between the large-scale predictor variables and local scale predictants. The statistical downscaling methods mainly include three types of methods: weather generator, transfer function and weather typing (Chen et al., 2012; Sharma et al., 2018). This study used the statistical downscaling model (SDSM) for downscaling. SDSM, developed by Rob Wilby and Christian Dawson in the UK, was one of the most popular statistical downscaling tools and can be best described as a hybrid of the stochastic weather generator and transfer function method (Hassan et al., 2013). The National Centers for Environmental Prediction (NCEP) reanalysis data was used to establish the statistical relationship between large-scale predictors and local scale predictands and calibrate the downscaling parameters. The calibrated downscaling parameters can be used for a scenario generator to produce different ensembles. The ensembles generated from SDSM can be considered as the uncertainty during statistical downscaling. Usually, the precipitation has a more significant impact on the surface runoff comparing temperature. Therefore, multiple ensembles (e.g., 20 ensembles) of precipitation and one ensemble of temperature were generated from H3A2a outputs for uncertainty analysis of downscaling results in this case.

2.3. Hydrological Modeling

In order to evaluate the propagated uncertainty effects, the well-behavioral hydrological modeling for the study area needs to be delivered first. The soil and water assessment tool (SWAT) model (Arnold et al., 1998), developed by the United States Department of Agriculture (USDA) Agricultural Research Service (ARS), was selected for surface runoff simulation in this study. SWAT requires specific information about weather, soil properties, topography, vegetation, and land management practices and is a physically based distributed model that operates on a daily time step for an ungauged watershed (Winchell et al., 2009). After the preparation required data inputs for SWAT and specific procedures for the calibration and validation, the hydrological model for certain study areas can be established. The case study was conducted by using the previous hydrological modeling case for the upstream of the Wenjing River watershed (Wu and Chen, 2015), and the calibrated model is considered as the well-expressed behavior model in this study.

2.4. Uncertainty Analysis

2.4.1. Indicators for Uncertainty Evaluation

The 95% prediction uncertainty (95PPU) was used to quantify and reflect surface runoff uncertainty. *P*-factor is used to quantify the degree of all uncertainties considered and is defined as the percentage of observed data bracketed the 95PPU. The *R*-factor is the measurement for evaluating the performance of uncertainty analysis and is obtained by the average distance of uncertainty bands divided by the standard deviation of the observed data. The larger *P*-factors are, the more observed data will fall in the 95PPU, demonstrating a high-fitted simulation performance; the smaller *R*-factors are, the narrower uncertainty bands (95PPU) will demonstrate less uncertainty. Therefore, simulations with relatively larger *P*-factor values and smaller *R*-factor values simultaneously are desired results. The *P*-factor and *R*-factor are calculated using the following equations (Abbaspour et al., 2007; Abbaspour, 2011; Xue et al., 2014; Wu and Chen, 2015):

$$P = \frac{nq_{in}}{N} \times 100\% \quad (1)$$

$$R = \frac{\overline{d_x}}{\sigma_x} \quad (2)$$

$$\overline{d_x} = \frac{1}{k} \times \sum_{l=1}^{k} (x_U - x_L)_l \quad (3)$$

where N is the total number of observed values, nq_{in} is the number of the observed data bracketed by 95PPU, σ_x is the standard deviation of the observed variable x, $\overline{d_x}$ is the average distance of the uncertainty band, l is a counter, k is the number of observed data for variable x, x_U and x_L is the upper and lower limit of the uncertainty band, respectively.

2.4.2. Uncertainty from Statistical Downscaling

In the real case study, using the statistical downscaled precipitation and temperature as the inputs of the SWAT model, a well-calibrated hydrological model was used to quantify the uncertainty propagated from statistical downscaling. Because the uncertainty from hydrological modeling was controlled by the optimized parameter set which achieves the largest NSE value from authors' previous study (Wu and Chen, 2015), the uncertainty generated from the application of different down-scaled ensembles can be considered as the uncertainty during applying the statistical downscaling method (SDSM). In this case, 20 downscaled precipitation ensembles can produce 20 simulations for surface runoff. After that, the NSE for the best simulation, 95PPU, *P*-factor, and *R*-factor can be calculated. The uncertainty evaluated in this step only comes from statistical downscaling.

2.4.3. Uncertainty from Hydrological Modeling

To avoid involving more uncertainties from hydrological modeling, the hydrological model was first calibrated using the sequential uncertainty fitting algorithm (SUFI-2) for two iterations. After two iterations using SUFI-2, all the parameter ranges have been reduced and adjusted to the optimal values. To comprehensively reflect the uncertainties of hydrological modeling, the 1,000 parameter sets sampled from parameter ranges in the third iteration of SUFI-2 using the Latin Hypercube Sampling (LHS) method were applied to simulate the surface runoff. While using observed meteorological data as input of the SWAT model, the 1,000 parameter sets can produce 1,000 surface runoff simulations. The associated NSE for the best simulation, 95PPU, *P*-factor, and *R*-factor can be calculated and considered as uncertainty from hydrological modeling only.

2.4.4. Total Uncertainty for Hydrological Modeling and Statistical Downscaling

To evaluate the propagated uncertainty effects during statistical downscaling, the total uncertainty, which includes the uncertainty from hydrological modeling and statistical downscaling in this study, was estimated. Precipitation is widely recognized as a key component of the hydrological cycle, exerting dominant effects on surface runoff (Tofiq and Guven, 2014; Berghuijs et al., 2017; Cheng et al., 2019; Ekwueme, 2022). After some trial studies and simulations, we have determined that the precipitation is far more sensitive than temperature to surface runoff in our case study. Therefore, as a preliminary attempt, we assume the uncertainty resulting from small variations in downscaled temperatures on surface runoff can be ignored, and we only focus on analyzing the uncertainty arising from variations in downscaled precipitation in this study. Consequently, only precipitation data has been down-scaled to different ensembles for uncertainty evaluation. The 20 ensembles of downscaled precipitation data and the downscaled mean maximum and minimum daily temperature were inputs for the SWAT model. The surface runoff simulation was conducted using different downscaled ensembles input combined with the 1,000 parameter sets generated from parameter ranges in the third iteration of SUFI-2 to evaluate the uncertainty propagation effects. Totally 20,000 simulations for surface runoff were done with the combinations of uncertainties from two sources. The best simulation for surface runoff and associated uncertainty indicators can be estimated afterwards.

3. Case Study

The proposed method was implemented in a real case study located on the upper reaches of the Wenjing River watershed with a drainage area equal to 653 km^2 located in Sichuan Province in western China (shown in Figure 2). The study area is about 25 km east of Chengdu, the capital city of Sichuan Province. The watershed was delineated and divided into 61

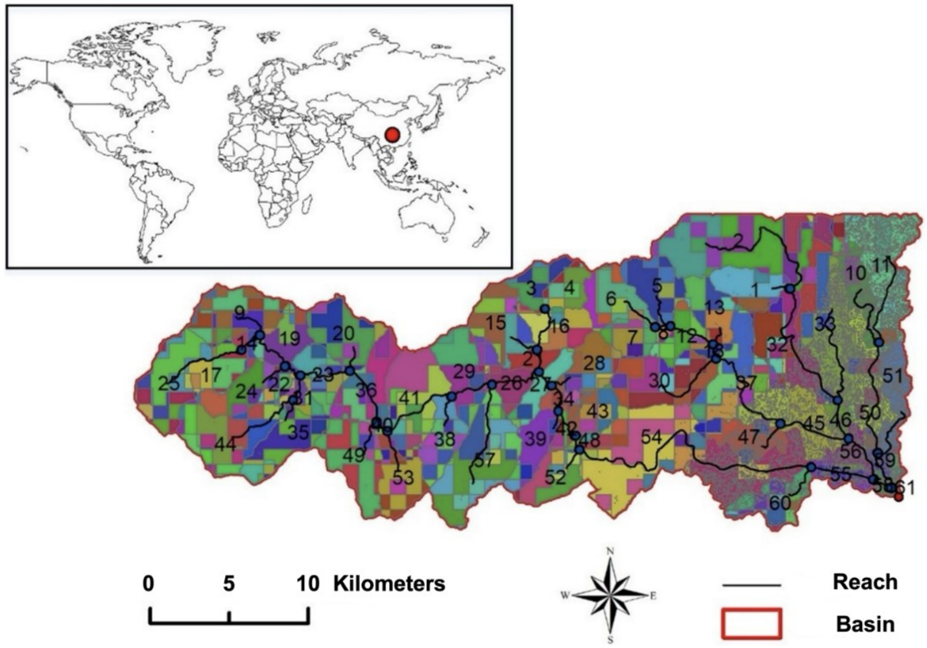

Figure 2. The location of the upstream of the Wenjing watershed.

sub-watersheds and 622 hydrologic response units (HRUs) using a 30 m resolution digital elevation model (DEM). The annual mean temperature is 15.9 °C, and the annual sunshine duration is 1,161.5 h. The report showed that the average annual precipitation is 1,012.4 mm (IWHR, 2005). The monthly streamflow data were available in the Yuantong station (the red dot in the watershed map in Figure 2), which is the outlet of the research watershed. The Wenjing River Watershed was selected as the study area due to its critical role as one of the primary water supplies for Chengdu (the capital and the most populous city in Sichuan province) and as an important water resource for irrigation in the downstream area. Managing water resources, particularly ensuring water safety, is of utmost importance for Chengdu. Moreover, the Wenjing River Watershed offers a naturally preserved environment with minimal human activities and artificial channels, making it an ideal setting for better performance of the hydrological simulation. Therefore, there has been increasing interest in conducting water resources management in this area (Wu and Chen, 2015).

4. Results and Discussion

4.1. Statistical Downscaling

As one of the most popular statistical downscaling tools, the SDSM model was selected for downscaling the precipitation and temperature data for this study. The NCEP reanalysis data were first applied to screen the sensitive predictor variables, and H3A2a data were applied later to obtain the downscaled ensembles for using hydrological runoff simulation to quantify the associated uncertainty. Twenty-six daily predictor variables for NCEP and H3A2a were considered. The definitions of each predictor variable are shown in Table 1. After the screening process in SDSM, ten important and sensitive predictor variables were selected in NCEP data; and these predictor variables were used to calibrate precipitation. Similarly, seven sensitive predictor variables of maximum daily temperature and five sensitive predictor variables of minimum temperature were screened, respectively. All the selected predictor variables for three different downscaling purposes are listed in Table 1. These predictor variables were used to generate the parameters for the regression model between daily weather data and regional-scale atmospheric variables in SDSM.

The observed precipitation and temperature data from 1980 to 2009 were obtained from the local meteorological department of the study area. However, the available NCEP reanalysis data was from 1961 to 2001, when the experiment was conducted. Therefore, due to the limitation of data availability, the 20-year data from 1981 to 2000 were divided into the calibration (1981 ~ 1995) and validation (1996 ~ 2000) period during downscaling. Figures 3(A) and 3(B) show the monthly mean downscaled precipitation using the NCEP reanalysis data and observed precipitation in the calibration and validation periods, respectively. Even though the overestimates for July and May in the validation were noticeable, the R^2 value showed acceptable results for the simulation. The R^2 value for downscaled monthly mean precipitation was 0.986 in the calibration period and 0.848 in the validation period, respectively. The seasonal precipitation results for the calibration and validation periods are shown in Figure 3(C) and 3(D). The long-term simulation results performed better than the monthly mean results. Although there were some overestimations in July for monthly mean precipitation for both the calibration and validation periods, the seasonal precipitation results were more balanced and well simulated.

After calibration and validation of downscaled precipita-

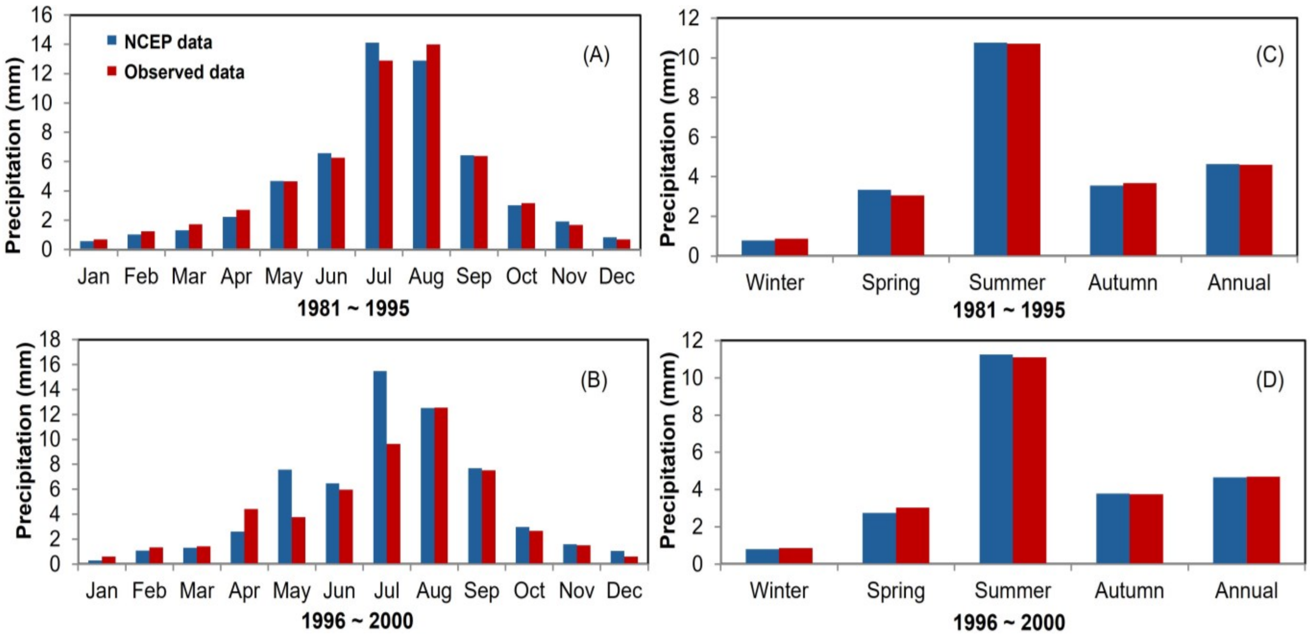

Figure 3. Monthly and seasonal means of observed and downscaled precipitations in the calibration (1981 ~ 1995) and validation (1996 ~ 2000) periods.

tion using the NCEP reanalysis data, due to the well-performed R^2 values, the H3A2a outputs can be downscaled using the regression parameters obtained from NCEP reanalysis data downscaling. In order to evaluate the uncertainty of precipitation, 20 synthetic ensembles were generated by using the H3A2a outputs in SDSM. The downscaled precipitation results were compared with observed data from 1981 to 1995, corresponding to the calibration period of the NCEP reanalysis data downscaling shown in Figure 4(A). The monthly mean of downscaled precipitation using the mean of 20 ensembles generated from H3A2a can achieve R^2 value of 0.760.

To investigate the uncertainty for the study period, the H3A2a outputs were downscaled for the same calibration and validation periods of the hydrological modeling study. According to available observed runoff data for hydrological simulation, five-year downscaled precipitation data (from 1998 ~ 2002) were compared with observed data. The 20 precipitation ensembles were used as input for the hydrological simulation using optimized parameter sets (which achieved the greatest NSE value using the observed meteorological data). The ensemble with the greatest NSE value of 0.67 for surface runoff simulation in SWAT can be viewed as the best-downscaled precipitation ensemble.

Figure 4(B) shows the observed and downscaled daily precipitation using the best-downscaled precipitation ensemble from H3A2a outputs. The precipitation downscaling was necessarily more problematic than temperature, especially for downscaling for the daily step. Typically, the precipitation was relatively poorly related to regional-scale predictors because both occurrence and amount needed to be specified, which were not suitable to be represented by constant relationships (Wilby et al., 2002). Therefore, the downscaling precipitation generally cannot achieve excellent results for most studies. Because the continuous surface runoff simulations were the desired results, the downscaled results, which can match observed data best for long-term periods, are expected. The downscaled monthly mean precipitation was calculated and applied for further analysis.

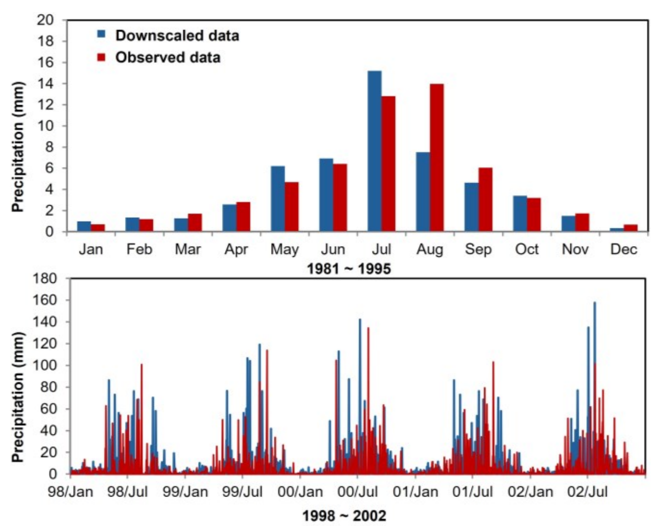

Figure 4. Observed and downscaled monthly mean and daily precipitations using the H3A2a model outputs.

Figure 5 shows the downscaled precipitation using the mean of 20 ensembles, the best-downscaled precipitation ensemble and observed precipitation. When using the mean of 20 ensembles and the best-downscaled precipitation ensemble from the 3A2a outputs, the R^2 values for monthly mean precipitation were 0.508 and 0.794, respectively. The overestimation in July and the underestimation in August remained the simulation from

Table 1. The Full List of Predictor Variables and Selected Predictor Variables for Precipitation and Temperature

Predictor Variable	Definition	Screened Predictor Variables Precipitation	Daily Maximum Temperature	Daily Minimum Temperature
ncepmslpas	Mean Sea Level Pressure			
ncepp_fas	Surface Airflow Strength			
ncepp_uas	Surface Zonal Velocity			
ncepp_vas	Surface Meridional Velocity			
ncepp_zas	Surface Vorticity			
ncepp_thas	Surface Wind Direction	Selected		
ncepp_zhas	Surface Divergence	Selected	Selected	
ncepp5_fas	500 hpa Airflow Strength	Selected		
ncepp5_uas	500 hpa Zonal Velocity		Selected	Selected
ncepp5_vas	500 hpa Meridional Velocity			
ncepp5_zas	500 hpa Vorticity	Selected		
ncepp5thas	500 hpa Wind Direction			
ncepp5zhas	500 hpa Divergence	Selected	Selected	
ncepp8_fas	850 hpa Airflow Strength	Selected		
ncepp8_uas	850 hpa Zonal Velocity	Selected		
ncepp8_vas	850 hpa Meridional Velocity			
ncepp8_zas	850 hpa Vorticity			Selected
ncepp8thas	850 hpa Wind Direction			
ncepp8zhas	850 hpa Divergence		Selected	
ncepp500as	500 hpa Geopotential Height	Selected	Selected	Selected
ncepp850as	850 hpa Geopotential Height			
ncepr500as	Relative Humidity at 500 hPa			
ncepr850as	Relative Humidity at 850 hPa	Selected		
ncephumas	Near Surface Relative humidity			
ncepshumas	Surface Specific Humidity	Selected	Selected	Selected
nceptempas	Mean Temperature at 2 m		Selected	Selected

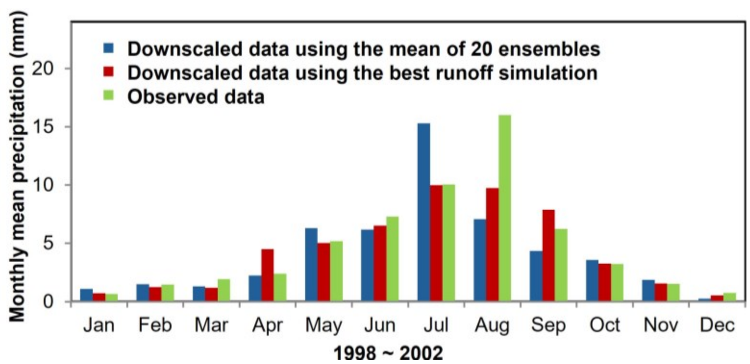

Figure 5. Monthly mean of observed, best downscaled, and mean of 20 downscaled ensembles precipitations using the H3A2a outputs from 1998 to 2002.

1981 to 1995, leading to the relatively low R^2 value. Even though the downscaled precipitation in July and August performed poorly, the downscaled results with the highest R^2 value for the long term (e.g., the year 1998 ~ 2002) were selected as desired results. To be noticed, if event-based hydrological models were used for hydrological simulations, seasonal or monthly downscaling and optimization may achieve better results for short-term simulation. In this study, although there were some overestimations in July and some underestimations in August for both the calibration and validation periods, the results can still be aplied to hydrological modeling due to the reasonable R^2 values and simulation requirement for monthly runoff.

Similarly, the maximum and minimum daily temperature data were downscaled using the same procedures. The NCEP reanalysis data were first used for screening parameters and calibration. The screened predictor variables for daily maximum and minimum temperatures were shown in Table 1. To better match the period of precipitation data as the input for the hydrological model, the temperature data was downscaled for the same period of downscaled precipitation. Based on the historical observed climate data, no extreme weather conditions or temperature anomalies were recorded during the simulated years in the study area. As mentioned earlier, given that small variations in temperature have limited effects on surface runoff, uncertainty from temperature will not be assessed in this study (however, we acknowledge that if temperature variations are too great or if many extreme events occur in the study areas, temperature uncertainty should be considered for more reliable results). Therefore, the mean of 20 temperature ensembles was used for the following analysis in this study.

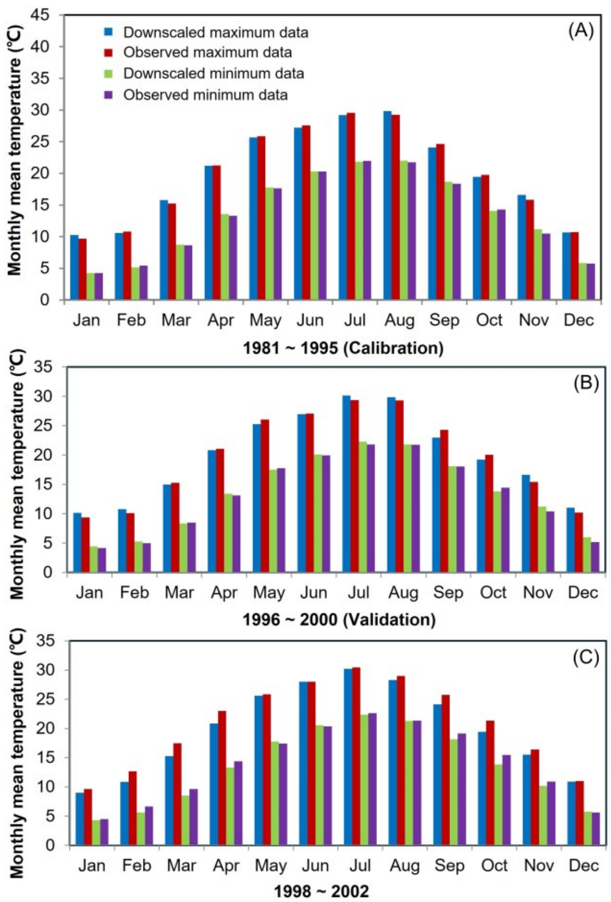

Figure 6. Monthly mean of observed and downscaled daily maximum and minimum temperature using the NCEP reanalysis data for (A) the calibration period (1981 ~ 1995) and (B) validation period (1996 ~ 2000), and (C) using the H3A2a outputs (1998 ~ 2002).

Figure 6(A) shows the monthly mean of observed and downscaled daily maximum and minimum temperature using NCEP reanalysis data from 1981 ~ 1995. The R^2 values for the monthly mean of daily maximum and minimum temperatures were 0.996 and 0.998 in the calibration period, respectively. For the validation period (from 1996 ~ 2000), the R^2 values of the monthly mean of daily maximum and minimum temperatures were 0.989 and 0.996, respectively, shown in Figure 6(B). As seen in Figure 6(A) and 6 (B), the monthly mean downscaled maximum and minimum temperatures matched the observed results well in both calibration and validation periods, indicating excellent downscaling performance for temperature by using SDSM. The H3A2a outputs were then applied to the calibrated regression parameters for downscaling.

Figure 7 shows the observed and downscaled daily maximum and minimum temperatures for the same calibration and validation period of hydrological modeling (1998 ~ 2002). The trends of observed and downscaled daily maximum and minimum temperatures were close and similar, although they need to match well for the daily step. If the performance of long-term simulation is the main interest, the temperature downscaling simulation performs well for the study period. Figure 6(C) shows the monthly mean of the observed and downscaled daily maximum and minimum temperature using H3A2a. The R^2 values for the monthly mean of daily maximum and minimum temperatures were 0.987 and 0.991, respectively, indicating the outstanding downscaling performance for temperatures in 1998 ~ 2002.

After downscaling the precipitation and temperature, two vital meteorological inputs of the SWAT model were prepared for hydrological simulations. As the precipitation had the dominant effect on surface runoff, 20 downscaled ensembles for precipitation were applied to the SWAT model for uncertainty analysis by evaluating the surface runoff simulation. As mentioned previously, due to small variations in temperature during the study periods, the uncertainty of the temperature was not considered in this study. The means of 20 downscaled ensembles' daily maximum and minimum temperatures were used as the temperature inputs of the SWAT model.

4.2. Hydrological Modeling

The SWAT model was first calibrated and validated using observed meteorological data for the study area. Our previous studies determined the most influential parameters through careful parameterization and calibration using the proposed multicriteria sequential calibration and uncertainty analysis (MS-CUA) method. The original parameters were selected according to the guidelines outlined in the SWAT manual and relevant literature. By using SUFI-2 and the proposed MS-CUA method, we determined the sensitivity of each parameter and removed insensitive parameters. After four iterations of MS-CUA, the parameter sets were optimized to achieve the best simulation performance. Moreover, the dramatically reduced parameter ranges can lead to a reduction in prediction uncertainties, increasing the reliability of simulation results. Since the simulations using the downscaled outputs were conducted during the same period as previous hydrological studies, the optimized parameter sets should remain valid for simulations using different meteorological inputs. Therefore, in this study, the key parameters are screened and selected based on the outcomes of previous studies (Wu and Chen, 2015; Wu et al., 2021).

The best simulation using observed meteorological data can achieve the NSE of 0.77 and R^2 of 0.80 for the calibration period and NSE of 0.74 and R^2 of 0.87 for the validation period for surface runoff simulation after three iterations using SUFI-2 (Wu and Chen, 2015). The parameter set of the best simulation can be viewed as the optimized parameter set. The exact values for each optimized parameter have been shown in Table 2. By

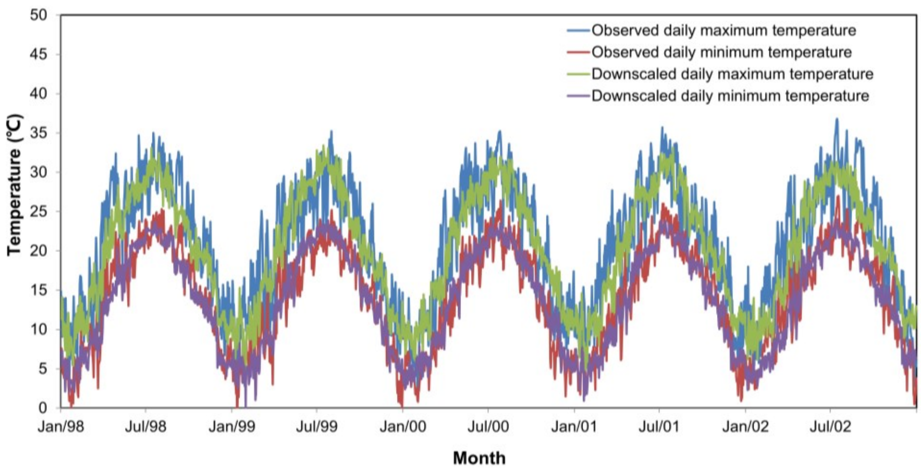

Figure 7. Observed and downscaled daily maximum and minimum temperature using the H3A2a outputs from 1998 to 2002.

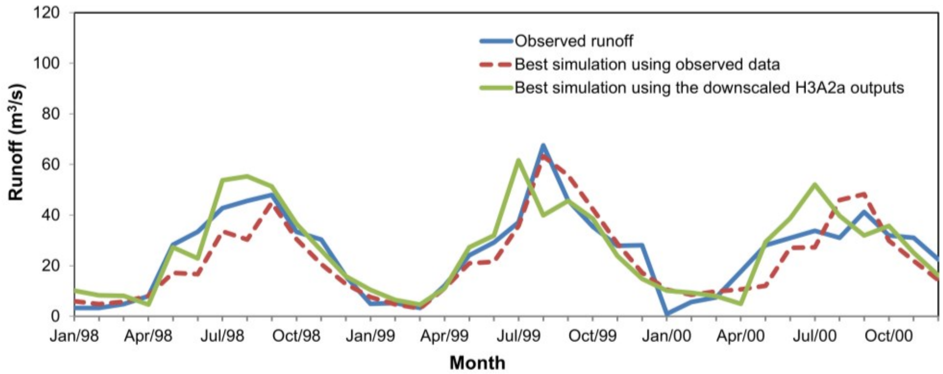

Figure 8. The hydrograph of the observed runoff, best simulation using observed meteorological and the downscaled H3A2a outputs.

using the optimized parameter set, all uncertainty during hydrological modeling has been fixed. If the uncertainty from different ensembles of meteorological data was involved, the uncertainty reflected by surface runoff should come from meteorological input data (which arise from statistical downscaling of the H3A2a outputs).

Table 2. The Exact Values of the Optimized Parameter Set

Parameters	Change Type	Optimized Parameter Values
CN_2	r	−0.258
ALPHA_BF	v	0.816
GW_DELAY	v	63.973
GWQMN	v	136.943
ESCO	v	0.987
CH_K	v	38.403
ALPHA_BNK	v	0.943
SOL_AWC	r	−0.165
SFTMP	v	5.169
GW_REVAP	v	0.022
RCHRG_DP	v	0.032

Note: "v"- replacing the existing parameter value; "r"- multiplying (1 + a given value) to the existing parameter value.

In comparing the simulation results and the calibrated runoff simulation results, the calibration period for hydrological modeling was selected as the study period from 1998 ~ 2000 for the uncertainty analysis. Figure 8 shows the hydrograph of the observed surface runoff, the best simulation after calibration using observed meteorological data and the best simulation using downscaled H3A2a outputs with optimized parameter sets of the SWAT model. The best surface runoff simulation using observed meteorological data after calibration can achieve the NSE of 0.77 and R^2 of 0.80. The simulation using best-downscaled H3A2a outputs can reach the NSE of 0.67 and R^2 of 0.73.

4.3. Uncertainty Analysis

During the hydrological simulations, each iteration included 1,000 sets for 11 parameters when conducting calibrations. The uncertainty of hydrological modeling considered in this study mainly came from applying different parameter sets. Figure 9(A) shows the uncertainty from hydrological modeling by applying different parameter sets. When uncertainty from statistical downscaling was considered, the optimal parameter set of the hydrological model was used, and the 95PPU of surface runoff was the propagated uncertainty from the application of different downscaled ensembles.

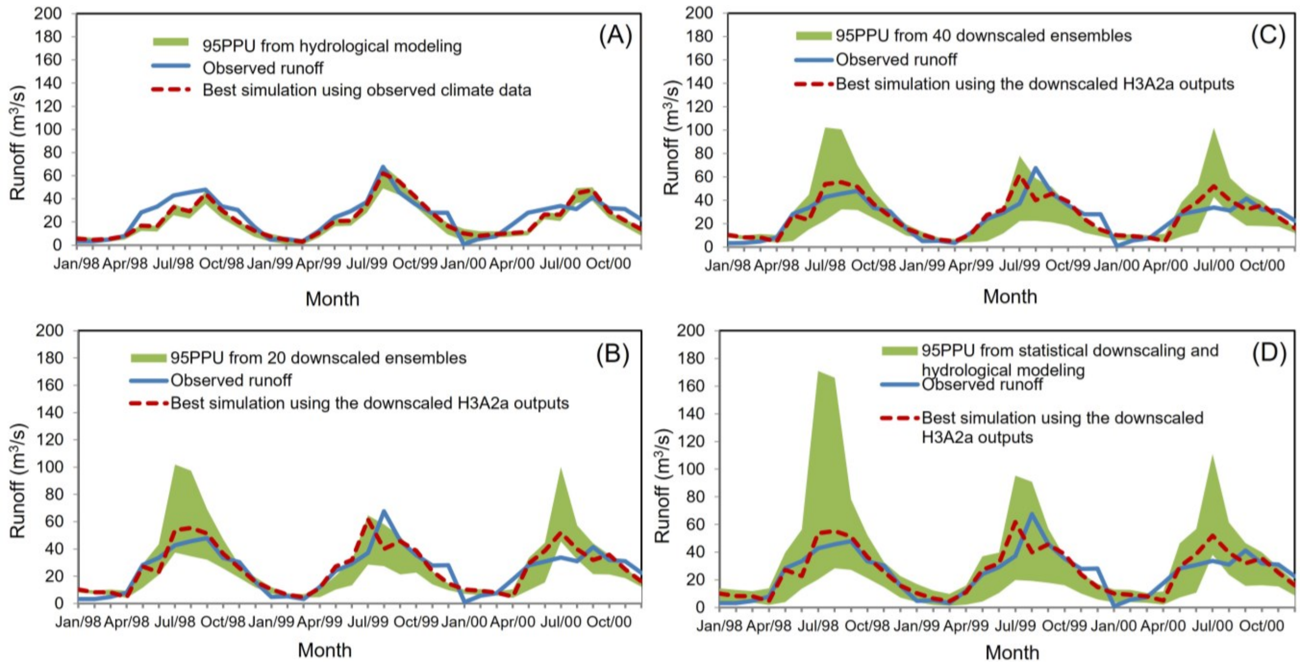

Figure 9. The hydrograph of the observed and best simulated runoff with 95PPU (A) from hydrological modeling, from downscaled H3A2a results using (B) 20 ensembles and (C) 40 ensembles, (D) generated from hydrological modeling and downscaled H3A2a outputs.

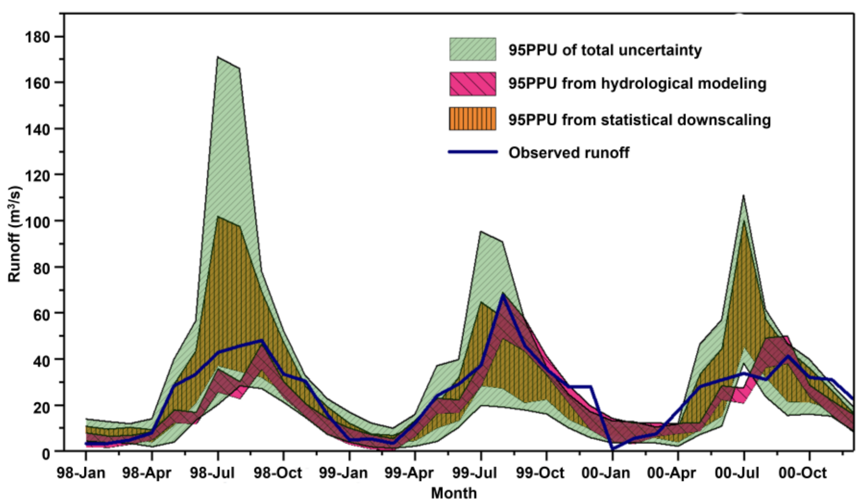

Figure 10. The observed runoff, 95PPU of total uncertainty, uncertainty from hydrological modeling, uncertainty from statistical downscaling.

The 10, 20, 30, 40, 50, and 60 downscaled precipitation ensembles were first generated using SDSM. The results showed that the uncertainty bands (95PPU) barely changed when ensembles were greater than 20. Figure 9(B) showed the uncertainty propagated from statistical downscaling using 40 downscaled ensembles. Figure 9(C) shows that the uncertainty of 20 downscaled ensembles represented an unnoticeable difference. As can be seen in Figures 9(B) and 9(C), the uncertainty from statistical downscaling produced much larger uncertainty bands than the uncertainty band from hydrological modeling (Figure 9(A)). The 95PPU using 40 downscaled ensembles produced a slightly higher uncertainty than the 95PPU generated using 20 downscaled ensembles but required more calculation resources. Since limited changes can be found for generating the 95PPU for the surface runoff by using different numbers of downscaled ensembles, 20 downscaled precipitation ensembles and the ensembles with the mean of 20 downscaled daily maximum and minimum temperatures were used for hydrological simulation for quantifying the uncertainty.

In this study, evaluating the total uncertainty, which included the uncertainty from hydrological modeling and statistical downscaling, was one of the primary tasks. Building on the ear-

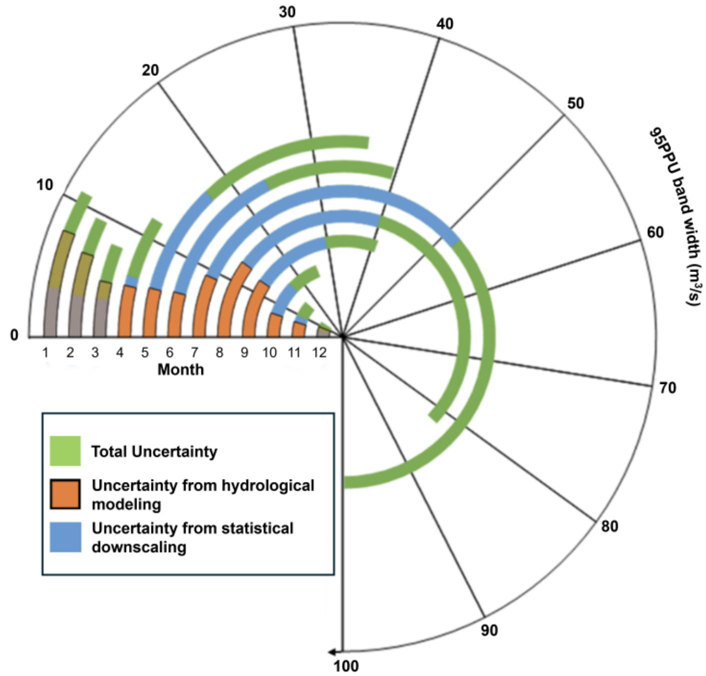

Figure 11. The uncertainty distribution of 95PPU of annual monthly surface runoff from different uncertainty sources.

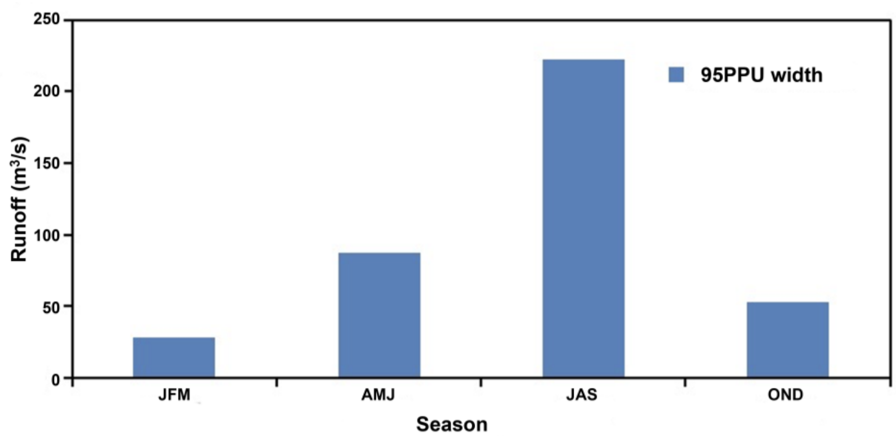

Figure 12. Annually seasonal mean width of 95PPU of the total uncertainty.

lier assumption (disregarding the uncertainty from temperature due to the negligible effects of small temperature variations on surface runoff), the uncertainty from hydrological modeling was represented by different parameter sets (1,000 sets), and the uncertainty from statistical downscaling was evaluated using different downscaled ensembles (20 ensembles of precipitation). Therefore, 20,000 simulations have been conducted to calculate the total uncertainty propagated from statistical downscaling to hydrological modeling. The uncertainty was reflected by using 95PPU of surface runoff. The 95PPU was calculated by using the lower level (at 2.5%) and upper level (at 97.5%) of the cumulative distribution of predicted surface runoff. Figure 9(D) shows the observed runoff, results of the best-simulated surface runoff and 95PPU of total uncertainty using the downscaled H3A2A outputs. As can be seen, the surface runoff during the peak flow period of the three years was much higher than the uncertainty of runoff in other seasons. Figure 9(D) also shows that the total uncertainty is more significant than individual uncertainties from two sources due to the broader uncertainty bands.

In order to show the propagation effects of the uncertainty clearly, the hydrograph (1998 ~ 2000) with uncertainty from different sources was shown in Figure 10. The green area was total uncertainty that stemmed from hydrological modeling and statistical downscaling. The brown area was the uncertainty arising from statistical downscaling only, and the pink area was the uncertainty from hydrological modeling only. In Figure 10, the pink area was much smaller than the brown area, indicating that the uncertainty effects from hydrological modeling are much smaller than from statistical downscaling to the surface runoff. Moreover, the brown and pink areas were smaller than the green areas, demonstrating that the total uncertainty was larger than the uncertainties from the two sources. However, the total uncertainty cannot be estimated with a simple addition of the two uncertainty sources, and the total uncertainty of surface flow was more considerable than the sum of the two uncertainty sources. The uncertainty from different sources can be easily quantified and compared to the *R*-factor values. The values of the *R*-factor of 95PPU for total uncertainty, uncertainty from statistical downscaling, and uncertainty from hydrological modeling were 2.03, 1.08, and 0.48, respectively. The larger the *R*-factor values indicated a higher level of uncertainty. When the relatively small uncertainty from statistical downscaling and hydrological modeling were combined for new hydrological simulations, the propagated uncertainty was much higher than the addition of the other two uncertainty sources. If the average width of 95PPU was used to evaluate the uncertainty, the total uncertainty was about 2.15 times of 95PPU from statistical downscaling and about 4.44 times of 95PPU from hydrological modeling on the monthly average. The extreme values of three 95PPU showed a significant difference in uncertainty effects. In 95PPU of total uncertainty band area, the largest peak flow could reach 171 m^3/s in July of 1998. In the same month, the largest flow of 95PPU from statistical downscaling and hydrological modeling were 101.8 m^3/s and 35.6 m^3/s. They were much smaller than the peak flow from 95PPU of the total uncertainty. The values of *P*-factor of 95PPU for total uncertainty, uncertainties from statistical downscaling, uncertainty from hydrological modeling were 0.75, 0.47 and 0.44, respectively. The broad uncertainty band still cannot cover all the observed surface runoff. It may be due to some unexpected human activities in the study watershed, such as summer irrigation and some small dams for electricity generation.

Figure 11 shows the 95PPU of the annual monthly surface runoffs from different uncertainty sources during 1998 ~ 2000. As seen in the figure, the uncertainty from hydrological modeling only took up a small portion of the total uncertainty, and the uncertainty from statistical downscaling made a higher contribution to the total uncertainty. Because the total uncertainty propagated from the uncertainty of statistical downscaling and hydrological modeling enlarged during the new simulations, the total uncertainty was much higher than the other two uncertainty sources. For example, in July, the 95PPU of total uncertainty was 1.92 times of uncertainty from statistical downscaling and 11.26 times of uncertainty from hydrological modeling; in August, the 95PPU of total uncertainty was 2.09 times of uncertainty from statistical downscaling and 6.17 times of uncertainty from hydrological modeling. These results demonstrates that new simulations dramatically increased propagated uncertainty when combining two uncertainty sources.

Also, the uncertainty of three different sources during the wet seasons (from May to Sep.) was much larger than the uncertainty in the dry season, which was indicated in Figure 12. The 95PPU of total uncertainty in the wet seasons (from May to Sep.) was 5.39 times of uncertainty in the dry seasons (from Jan. to Apr. and from Oct. to Dec.) during the three years.

As shown in Figure 12, if the seasonal results were concerned, the total uncertainty effects on the four seasons were not evenly distributed. The first season, including Jan., Feb., and Mar. (JFM), had the smallest 95PPU in all three years with an average bandwidth of 28.1 m^3/s; the second season, including Apr., May, and Jun. (AMJ), had the second largest average uncertainty bandwidth of 86.9 m^3/s in three years; the third season, including Jul., Aug., Sep. (JAS), had the most massive average uncertainty band in three years with the value of 222.4 m^3/s; and the last season, including Oct., Nov., Dec. (OND), had the third-largest average uncertainty bandwidth which is 53.6 m^3/s in all three years. As shown in Figure 11, the summer season (JAS) had the greatest total uncertainty compared with the other three seasons. The dry season of each year showed less variation and uncertainty in the study area. The reason for that could be concluded that the less uncertainty of surface runoff was mainly caused by less variation of downscaled GCM outputs (especially downscaled precipitation) during the dry season.

5. Conclusions

Due to the lack of methods for quantitatively evaluating propagated uncertainty effects from statistical downscaling and hydrological modeling, this study proposed the ISES-UPA method to address this gap. To demonstrate the feasibility of the method, a case study in the upstream of the Wenjing River Watershed in Sichuan, China, was conducted. Initially, using statistical methods (SDSM), the precipitation and temperature data were downscaled using the Hadley Centre Coupled Model 3 (HadCM3) for the A2 scenario (H3A2a). Recognizing the significance and sensitivity of precipitation to hydrological simulation output, the uncertainty of precipitation was considered the sole uncertainty source of statistical downscaling in this study. The uncertainty of precipitation was reflected by applying different downscaled precipitation ensembles as the input of the hydrological modeling. The uncertainty arising from statistical downscaling and hydrological modeling was evaluated separately first, and then the combined uncertainty effects were evaluated using 95PPU of the surface runoff.

The results revealed that the total propagated uncertainty significantly exceeds the simple addition of the other two uncertainty sources. Figures 10 and 11 depict the uncertainty effects from the three individual sources. Although the uncertainty effects from statistical downscaling alone and hydrological modeling alone were relatively small, the propagated uncertainty experienced a significant amplification when combining two uncertainty sources for new hydrological simulations. If the average width of 95PPU was used to evaluate the uncertainty, the total uncertainty was about 2.15 times of 95PPU from statistical downscaling and about 4.44 times of 95PPU from hydrological modeling on the monthly average. Additionally, the findings also indicated that the uncertainty of surface runoff during the wet season exhibited a higher level of uncertainty compared to the dry season (e.g., 5.39 times greater than the dry season).

Through the implementation of the proposed ISES-UPA method, this study performed a quantitative assessment of uncertainty propagation effects. It systematically compared and quantified the uncertainty arising from both statistical downscaling and hydrological modeling, as well as the total enlarged uncertainty from these two uncertainty sources. The findings from this study can serve as valuable scientific references for water resource management in the study area. When applying future climate scenarios to make critical decisions, the total propagated uncertainty information could provide decision-makers with great confidence in mitigating the potential risks and damages caused by extreme events. Overall, this research significantly contributes to addressing key gaps in understanding uncertainty propagation effects, providing a robust methodological framework for future hydro-meteorological studies. For future research, the proposed method is ready to evaluate uncertainty propagation effects when more sources of uncertainty are introduced to the system. The contributions of each uncertainty component could be calculated and shown in hydrographs for comparison using the proposed method. The limited availability of observed data for calibration and validation may impact the reliability of analysis results. Enhancing the application by incorporating more observed data, high-resolution data, multiple hydrological models, and exploring multiple study areas can further improve the understanding of uncertainty propagation effects.

Acknowledgements. The research work was supported by Natural Sciences and Engineering Research Council of Canada (NSERC), Canada Foundation for Innovation (CFI), and United Nations Development Programme.

References

Abbaspour, K.C. (2011). *SWAT-CUP4: SWAT Calibration and Uncertainty Programs - A User Manual*. Swiss Federal Institute of Aquatic Science and Technology, Switzerland.

Abbaspour, K.C., Yang, J., Maximov, I., Siber, R., Bogner, K., Mieleitner, J., Zobrist, J. and Srinivasan, R. (2007). Modelling hydrology and water quality in the pre-alpine/alpine Thur watershed using SWAT. *J. Hydrol*., 333(2-4), 413-430. https://doi.org/10.1016/j.jhdrol.2006.09.014

Ahmadalipour, A., Moradkhani, H. and Rana, A. (2018). Accounting for downscaling and model uncertainty in fine-resolution seasonal climate projections over the Columbia River Basin. *Clim. Dynam*., 50, 717-733. https://doi.org/10.1007/s00382-017-3639-4

Anteneh, Y., Alamirew, T., Zeleke, G. and Kassawmar, T. (2023). Modeling runoff-sediment influx responses to alternative BMP interventions in the Gojeb watershed, Ethiopia, using the SWAT hydrological model. *Environ. Sci. Rollut. R.*, 30, 22816-22834. https://doi.org/10.1007/s11356-022-23711-4

Arnold, J.G., Srinivasan, R., Muttiah, R.S. and Williams, J.R. (1998). Large area hydrologic modeling and assessment Part I: Model development. *J. Am. Water Resour. Assoc.*, 34(1), 73-89. https://doi.org/10.1111/j.1752-1688.1998.tb05961.x

Bennett, K.E., Werner, A.T. and Schnorbus, M. (2012). Uncertainties in hydrologic and climate change impact analyses in headwater basins of British Columbia. *J. Climate*., 25(17), 5711-5730. https://doi.org/10.1175/JCLI-D-11-00417.1

Berghuijs, W.R., Larsen, J.R., Van Emmerik, T.H. and Woods, R.A. (2017). A global assessment of runoff sensitivity to changes in precipitation, potential evaporation, and other factors. *Water Resour. Res.*, 53(10), 8475-8486. https://doi.org/10.1002/2017WR021593

Bosshard, T., Carambia, M., Goergen, K., Kotlarski, S., Krahe, P., Zappa, M. and Schär, C. (2013). Quantifying uncertainty sources in an ensemble of hydrological climate-impact projections. *Water Resour. Res*., 49(3), 1523-1536. https://doi.org/10.1029/2011WR011533

Bui, L.T. and Pham, H.T.H. (2023). Linking hydrological, hydraulic and water quality models for river water environmental capacity assessment. *Sci. Total Environ*., 857(2), 159490. https://doi.org/10.1016/j.scitotenv.2022.159490

Chadwick, R., Coppola, E. and Giorgi, F. (2011). An artificial neural network technique for downscaling GCM outputs to RCM spatial scale. *Nonlinear Proc. Geoph*., 18(6), 1013-1028. https://doi.org/10.51 94/npg-18-1013-2011

Chaudhuri, C. and Srivastava, R. (2017). A novel approach for statistical downscaling of future precipitation over the Indo-Gangetic Basin. *J. Hydrol*., 547, 21-38. https://doi.org/10.1016/j.jhdrol.2017.01. 024

Chen, B., Jing, L., Zhang, B. and Liu, S. (2011). Wetland monitoring, characterization and modelling under changing climate in the Canadian Subarctic. *J. Environ. Inform*., 18(2), 55-64. https://doi.org/10.3808/jei. 201100199

Chen, J., Brissette, F.P. and Leconte, R. (2012). Coupling statistical and dynamical methods for spatial downscaling of precipitation. *Climatic Change*, 114(3-4), 509-526. https://doi.org/10.1007/s105 84-0 12-0452-2

Chen, X. and Niu, J. (2020). Evaluating the adaptation of Chinese Torreya plantations to climate change. *Atmosphere*, 11(2), 176. https://doi.org/10.3390/atmos11020176

Cheng, L., Ma, L., Yang, M., Wan, G. and Wang, X. (2019). Changes of temperature and precipitation and their impacts on runoff in the upper Taohe River in northwest China from 1956 to 2014. *Environ. Earth Sci*., 78(14), 1-14. https://doi.org/10.1007/s12665-019-8399-5

Dai, A., Rasmussen, R.M., Ikeda, K. and Liu, C. (2020). A new approach to construct representative future forcing data for dynamic downscaling. *Clim. Dyn.*, 55, 315-323. https://doi.org/10.1007/s00382-017-3708-8

Dang, T.D., Chowdhury, A.K. and Galelli, S. (2020). On the representation of water reservoir storage and operations in large-scale hydrological models: implications on model parameterization and climate change impact assessments. *Hydrol. Earth Syst. Sc*., 24, 397-416. https://doi.org/10.5194/hess-24-397-2020

DeFries, R.S., Townshend, J.R. and Los, S.O. (2023). Scale in remote sensing and GIS. *Scaling Land Cover Heterogeneity for Global Atmosphere–Biosphere Models*. Routledge Publishing, pp 231-246. https://doi.org/10.1201/9780203740170

Dong, S., Yu, T., Farahmand, H. and Mostafavi, A. (2020). Bayesian modeling of flood control networks for failure cascade characterization and vulnerability assessment. *Comput.-Aided Civ. Inf*., 35(7), 668-684. https://doi.org/10.1111/mice.12527

Ekwueme, B.N. (2022). Machine learning based prediction of urban flood susceptibility from selected rivers in a tropical catchment area. *Civil Eng*., 8(9), 1857. http://dx.doi.org/10.28991/CEJ-2022-08-09-08

Fallah, A. and Orth, R. (2020). Climate-dependent propagation of precipitation uncertainty into the water cycle. *Hydrol. Earth Syst. Sc.*, 24(7), 3725-3735. https://doi.org/10.5194/hess-24-3725-2020

Gudmundsson, L. (2012). *Assessing the Suitability of Weather Generators Based on Generalised Linear Models for Downscaling Climate Projections*. Norwegian Meteorological Institute, Norway.

Hassan, Z., Shamsudin, S. and Harun, S. (2013). Application of SDSM and LARS-WG for simulating and downscaling of rainfall and temperature. *Thero. Appl. Climatol.*, 116, 243-257. https://doi.org/10.1007/s00704-013-0951-8

Her, Y., Yoo, S.H., Cho, J., Hwang, S., Jeong, J. and Seong, C. (2019). Uncertainty in hydrological analysis of climate change: Multi-parameter vs. multi-GCM ensemble predictions. *Sci. Rep*., 9, 1-22. https://doi.org/10.1038/s41598-019-41334-7

IPCC. (2007). *Fourth Assessment Report, Climate Change*. Cambridge University Press, Cambridge.

IWHR. (2005). *Investigation on Current Drinking Water Supply Mechanism in Chongzhou.* China Institute of Water Resources and Hydropower Research, Beijing.

Jin, G., Chen, K., Wang, P., Guo, B., Dong, Y. and Yang, J. (2019). Trade-offs in land-use competition and sustainable land development in the North China Plain. *Technol. Forecast Soc*., 141, 36-46. https://doi.org/10.1016/j.techfore.2019.01.004

Jing, L., Chen, B., Ye, X. and Zhang, B. (2017). Wastewater treatment plant network design using a multiscale two-stage mixed integer stochastic model. *Environ. Eng. Sci.*, 34(12), 861-871. https://doi.org/10. 1089/ees.2017.0100

Krysanova, V., Vetter, T., Eisner, S., Huang, S., Pechlivanidis, I., Strauch, M., Gelfan, A., Kumar, R., Aich, V. and Arheimer, B. (2017). Intercomparison of regional-scale hydrological models and climate change impacts projected for 12 large river basins worldwide – A synthesis. *Environ. Res. Lett.*, 12(10), 105002. https://doi.org/10.1088/17489326/aa8359

Li, Z., Chen, B., Wu, H., Ye, X. and Zhang, B. (2018). A design of experiment aided stochastic parameterization method for modeling aquifer NAPL contamination. *Environ. Modell. Softw.*, 101, 183-193. https://doi.org/10.1016/j.envsoft.2017.12.014

Lindenschmidt, K. and Rokaya, P. (2019). A stochastic hydraulic modelling approach to determining the probable maximum staging of Ice-Jam floods. *J. Environ. Inform.*, 34(1), 45-54. https://doi.org/10.3808/jei.201900416

Lu, W., Qin, X. and Jun, C. (2019). A parsimonious framework of evaluating WSUD features in urban flood mitigation. *J. Environ. Inform.*, 33(1), 17-27. https://doi.org/10.3808/jei.201700373

Lucas-Picher, P., Arsenault, R., Poulin, A., Ricard, S., Lachance Cloutier, S. and Turcotte, R. (2020). Application of a high - resolution distributed hydrological model on a US-Canada transboundary basin: Simulation of the multiyear mean annual Hydrograph and 2011 flood of the Richelieu River Basin. *J. Adv. Model. Earth. Syst.*, 12(4). https://doi.org/10.1029/2019MS001709

Maurya, S., Srivastava, P.K., Zhuo, L., Yaduvanshi, A. and Mall, R. (2023). Future climate change impacts on the streamflow of Mahi River basin under different general circulation model scenarios. *Water Resour. Manag.*, 37, 2675-2696. https://doi.org/10.1007/s11269-022-03372-1

McMillan, H.K., Westerberg, I.K. and Krueger, T. (2018). Hydrological data uncertainty and its implications. *WIRES. Water.*, 5, e1319. https:// doi.org/10.1002/wat2.1319

Mei, H., Li, Y., Lv, J., Chen, X., Lu, C., Suo, C. and Ma, Y. (2021). Development of an integrated method (MGCMs-SCA-FER) for assessing the impacts of climate change–A case study of Jing-Jin-Ji region. *J. Environ. Inform.*, 38(2), 145-161. https://doi.org/10.3808/jei.202100458

Miao, C., Wu, Y., Fan, X. and Su, J. (2023). Projections of global land runoff changes and their uncertainty characteristics during the 21st century. *Earth's Future*, 11(4). https://doi.org/10.1029/2022EF003286

Nakicenovic, N., Alcamo, J., Davis, G., Vries, B.d., Fenhann, J., Gaffin, S., Gregory, K., Grubler, A., Jung, T.Y. and Kram, T. (2000). *Special Report on Emissions Scenarios*. Cambridge University Press, Cambridge.

Nourani, V., Jabbarian Paknezhad, N., Sharghi, E. and Khosravi, A. (2019). Estimation of prediction interval in ANN-based multi-GCMs downscaling of hydro-climatologic parameters. *J. Hydrol.*, 579(1-2), 124226. https://doi.org/10.1016/j.jhydrol.2019.124226

Rakhimova, M., Liu, T., Bissenbayeva, S., Mukanov, Y., Gafforov, K.S., Bekpergenova, Z. and Gulakhmadov, A. (2020). Assessment of the impacts of climate change and human activities on runoff using climate elasticity method and general circulation model (GCM) in the Buqtyrma River Basin, Kazakhstan. *Sustainability*, 12(12), https://doi.org/10.3390/su12124968

Rodríguez, E., Sánchez, I., Duque, N., Arboleda, P., Vega, C., Zamora, D., López, P., Kaune, A., Werner, M. and García, C. (2019). Combined use of local and global hydro meteorological data with hydrological models for water resources management in the Magdalena-Cauca Macro Basin – Colombia. *Water Resour. Manag.*, 34, 2179-2199. https://doi.org/10.1007/s11269-019-02236-5

Sa'adi, Z., Shiru, M.S., Shahid, S. and Ismail, T. (2020). Selection of general circulation models for the projections of spatio-temporal changes in temperature of Borneo Island based on CMIP5. *Theor. Appl. Climatol.*, 139(2000), 351-371. https://doi.org/10.1007/s00704-019-02948-z

Samadi, S., Carbone, G., Mahdavi, M., Sharifi, F. and Bihamta, M. (2012). Statistical downscaling of climate data to estimate streamflow in a semi-arid catchment. *Hydrol. Earth Syst. Sci.*, 9, 4869-4918. https://doi.org/10.5194/hessd-9-4869-2012

Sharma, T., Vittal, H., Chhabra, S., Salvi, K., Ghosh, S. and Karmakar, S. (2018). Understanding the cascade of GCM and downscaling uncertainties in hydro-climatic projections over India. *Int. J. Climatol.*, 38(S1), e178-e190. https://doi.org/10.1002/joc.5361

Shen, M., Chen, J., Zhuan, M., Chen, H., Xu, C.Y. and Xiong, L. (2018). Estimating uncertainty and its temporal variation related to global climate models in quantifying climate change impacts on hydrology. *J. Hydrol.*, 556, 10-24. https://doi.org/10.1016/j.jhydrol.2017.11.004

Shrestha, N. and Wang, J. (2020). Water quality management of a cold climate region watershed in changing climate. *J. Environ. Inform.*, 35(1), 59-80. https://doi.org/10.3808/jei.201900407

Tapiador, F.J., Navarro, A., Moreno, R., Sánchez, J.L. and García-Ortega, E. (2020). Regional climate models: 30 years of dynamical downscaling. *Atmos. Res.*, 235, 104785. https://doi.org/10.1016/j.atmosres.2019.104785

Tian, X., An, C. and Chen, Z. (2020). Assessing the impact of urban form on the greenhouse gas emissions from household vehicles: A review. *J. Environ. Inform. Lett.*, 3(2), 70-85. https://doi.org/10.3808/jeil.202000029

Tofiq, F. and Guven, A. (2014). Prediction of design flood discharge by statistical downscaling and General Circulation Models. *J. Hydrol.*, 517, 1145-1153. https://doi.org/10.1016/j.jhdrol.2014.06.028

Trolle, D., Nielsen, A., Andersen, H.E., Thodsen, H., Olesen, J.E., Børgesen, C.D., Refsgaard, J.C., Sonnenborg, T.O., Karlsson, I.B., and Christensen, J.P. (2019). Effects of changes in land use and climate on aquatic ecosystems: Coupling of models and decomposition of uncertainties. *Sci. Total Environ.*, 657, 627-633. https://doi. org/10.1016/j.scitotenv.2018.12.055

Van Beusekom, A.E., Gould, W.A., Terando, A.J. and Collazo, J.A. (2016). Climate change and water resources in a tropical island system: propagation of uncertainty from statistically downscaled climate models to hydrologic models. *Int J. Climatol.*, 36(9), 3370-3383. https://doi.org/10.1016/10.1002/joc.4560

Vetter, T., Reinhardt, J., Flörke, M., van Griensven, A., Hattermann, F., Huang, S., Koch, H., Pechlivanidis, I.G., Plötner, S. and Seidou, O. (2017). Evaluation of sources of uncertainty in projected hydrological changes under climate change in 12 large-scale river basins. *Climatic Change*, 141, 419-433. https://doi.org/10.1007/s10584-016-1794-y

Warmink, J.J., Janssen, J., Booij, M.J. and Krol, M.S. (2010). Identification and classification of uncertainties in the application of environmental models. *Environ. Modell. Softw.*, 25(12), 1518-1527. https://doi.org/10.1016/j.envsoft.2010.04.011

Wilby, R.L., Dawson, C.W. and Barrow, E.M. (2002). SDSM-a decision support tool for the assessment of regional climate change impacts. *Environ. Modell. Softw.*, 17(2), 145-157. https://doi.org/10.1016/ S1364-8152(01)00060-3

Winchell, M., Srinivasan, R., Luzio, M.D. and Arnold., J. (2009). *ARCSWAT 2.3.4 Interface for SWAT2005*. Grassland, soil and water research service, Texas, the United States.

Wu, H. and Chen, B., (2014). Uncertainty analysis for propagation effects from statistical downscaling to hydrological modeling. *Advances in International Conference on Marine and Freshwater Environ-ments (iMFE)*, St. John's, Newfoundland, CA.7

Wu, H. and Chen, B. (2015). Evaluating uncertainty estimates in distributed hydrological modeling for the Wenjing River watershed in China by GLUE, SUFI-2, and ParaSol methods. *Ecol. Eng.*, 76, 110-121. https://doi.org/10.1016/j.ecoleng.2014.05.014

Wu, H., Chen, B. and Li, P. (2013). Comparison of sequential uncertainty fitting algorithm (SUFI-2) and parameter solution (ParaSol) method for analyzing uncertainties in distributed hydrological modeling–A Case Study. *Canadian Society for Civil Engineering (CSCE) 2013 General Conference*. Montréal, Québec, *GEN*, *309*(1).

Wu, H., Chen, B., Snelgrove, K. and Lye, L. (2019). Quantification of uncertainty propagation effects during statistical downscaling of precipitation and temperature to hydrological modeling. *J. Environ. Inform.*, 2(34), 139-148. https://doi.org/10.3808/jei.201600347

Wu, H., Chen, B., Ye, X., Guo, H., Meng, X. and Zhang, B. (2021). An improved calibration and uncertainty analysis approach using a multicriteria sequential algorithm for hydrological modeling. *Sci. Rep.*, 11, 16954. https://doi.org/10.1038/s41598-021-96250-6

Xue, C., Chen, B. and Wu, H. (2014). Parameter uncertainty analysis of surface flow and sediment yield in the Huolin Basin, China. *J. Hydrol. Eng.*, 19(6), 1124-1236. https://doi.org/10.1061/(ASCE)HE.1 943-5584.000090

Yang, G., Li, M. and Guo, P. (2022). Monte carlo-based agricultural water management under uncertainty: a case study of Shijin Irrigation District, China. *J. Environ. Inform.*, 39(2), 152-164. https://doi.org/10.3808/jei.202000441

Zhang, D., Lin, Q., Yao, H., He, Y., Deng, J. and Zhang, X. (2021). Accelerating SWAT simulations using an in-memory NoSQL database. *J. Environ. Inform.*, 37(2), 142-152. https://doi.org/10.3808/jei.2019 00425

Zhu, X., Zhang, A., Wu, P., Qi, W., Fu, G., Yue, G. and Liu, X. (2019). Uncertainty impacts of climate change and downscaling methods on future runoff projections in the Biliu River Basin. *Water*, 11(10), 2130. https://doi.org/10.3390/w11102130